J Low Temp Phys (2008) 153: 103–122
DOI 10.1007/s10909-008-9821-7

Current-Temperature Diagram of Resistive States in Long Superconducting Niobium Filaments

F.-R. Ladan · K. Harrabi · M. Rosticher · P. Mathieu · J.-P. Maneval · C. Villard

Received: 22 July 2008 / Accepted: 14 August 2008 / Published online: 1 October 2008

Abstract By applying nanosecond current pulses to narrow superconducting Nb strips, we have observed the induced resistive states expected for quasi 1-D transport, namely localized phase-slip centres (PSC) and hot spots (HS). The current-controlled drive discriminates stable-in-time PSC structures near T_c from expanding HS at lower temperatures. HS-PSC exchange and return towards equilibrium are studied by using two-step current pulses. Remarkably, it appears that a hot spot never forms unless a PSC has first been nucleated. Then from a plot of the threshold currents $I_c(T)$ and $I_h(T)$, corresponding to PSC and HS, respectively, one can predict the response to current, temperature, or luminous excitation, as well as the effect of an applied magnetic field.

Keywords Niobium · Phase slip centres · Hot spots · Superconducting thin films

PACS 74.40.+k · 74.50.+r · 06.60.Jn · 74.76.Db

1 Introduction

In sufficiently narrow filaments or strips, the current-induced breakdown of superconductivity is concentrated into one or several zones of micrometric length, whatever the uniformity of the device. Such dissipation units, distinct from the thermally-activated phase-slip events, have been interpreted as phase-slips centres (PSCs), in which oscillation of the order parameter allows the phase differences to relax by

F.-R. Ladan · K. Harrabi · M. Rosticher · P. Mathieu · J.-P. Maneval (✉)
Ecole Normale Supérieure, Laboratoire de Physique LPA, 24 rue Lhomond, 75231 Paris 5, France
e-mail: maneval@lpa.ens.fr

C. Villard
CNRS, Institut NÉEL, 25 rue des Martyrs, BP 166, 38042 Grenoble 9, France

quanta of 2π [1, 2]. They were observed first as steps in the resistance *vs* temperature $R(T)$ transition of tin whiskers [3], and then found also in the current-voltage (I–V) characteristic curves of whiskers [4] and of microstrips [4, 5]. Once considered as typical manifestations of one-dimensional (1-D) superconductivity, which implies transverse dimensions not exceeding the coherence length ξ, PSCs have since been generalized into phase-slip lines for wide strips [6], and they have been observed in a number of materials and under various physical conditions.

In this work the critical current I_c refers to the threshold for PSC nucleation, and the corresponding current density is written J_c. When the current increases significantly larger than I_c, the PSC naturally evolves [7] into an ordinary normal zone, or hot spot (HS), with an internal temperature larger than the critical temperature T_c. Let us call I_h the related threshold current, whose Joule effect is sufficient to maintain a *localized* normal zone above T_c. On lowering the bath temperature T_b, the more abrupt increase of I_c compared to that of I_h reverses the situation, and thus places $I_c(T_b)$ above $I_h(T_b)$. In this case, the low-T resistive response observed experimentally is that of a HS [5, 7]. Since the filament is initially non-dissipative, this raises the question of the mechanism (temperature fluctuations, defects at contacts, ...) able to initiate the HS behaviour, assuming the sample has been cooled with zero applied current. The aim of this paper is to develop a semi-quantitative framework for predicting the formation of one or the other of the current-driven resistive modes (PSC or HS) through the functional dependences $I_c(T)$ and $I_h(T)$, and interpreting the response to adjustable external actions, such as the application of a magnetic field or irradiation by light (Sects. 6, 7).

Previous studies [3–5] identified a PSC mostly from its resistance jump, its "excess" non-dissipative current, and its constant differential resistance on dc-current I–V plots. More sophisticated techniques, using a set of voltage probes arranged on the micrometer scale [8], radio-frequency synchronization [5, 9], or laser-imaging [6], have led to deeper physical understanding. In Sect. 4, we distinguish PSCs from other resistive processes, such as vortex-flow (VF) or faulty electrical connections, by their characteristic delay time for nucleation after a pulsed electrical excitation [10]. *A constant current-controlled drive* proves essential in singling out HSs from PSCs from their temporal behaviour. We then observe the return of a given resistive state to another one of lower current, and draw the I–T diagram of a given sample (Sect. 5).

The PSC regime has often been considered [3–5] as confined to a small temperature range, a tiny fraction of a kelvin below T_c. We challenge this assertion in the present work, and find its range of validity to be much more extended in niobium, confirming earlier observations [9]. This raises the question of the elevation of temperature at the PSC site [11]. In an Appendix, we sketch a computation of that quantity, for PSC or HS, as governed by the film-to-substrate thermal coupling coefficient introduced in this work.

2 1-D Resistive States and Their Expected I–T Diagram

The response of a one-dimensional superconducting filament to a current larger than I_c, the *depairing*, or Ginzburg-Landau, critical current ((4.36) in [1]), is the PSC,

where the pair-wave function periodically decays to zero and reforms [2]. Out of the total current, on the time average, a fraction I_S, (of order $I_c/2$), passes through without dissipation. In this respect, a PSC belongs to the superconducting state. This picture leads, in an I–V plot, to a voltage jump at I_c followed by an ascending ramp of the form $V = R_u(I - I_S)$, where R_u and the "excess current" I_S are, in first approximation, independent of the current I. The differential resistance R_u arises from the quasiparticles liberated at each closure of the gap and diffusing on both sides of the proper phase-slip zone, of extension ξ, over a characteristic length $\Lambda = (v_F l_e \tau_R/3)^{1/2}$, where v_F is the Fermi velocity, and l_e is the electronic mean free path. In the standard SBT model [5], τ_R is the branch imbalance, or "transverse", relaxation time, of the order of magnitude of the inelastic electron lifetime τ_E, except close to T_c where it diverges like $(1-t)^{1/2}$ [11]. (Here t is the reduced temperature T/T_c.) Values such as $l_e = 5$ nm, $\tau_E = 200$ ps, put the equivalent normal resistive length 2Λ in the micrometer range, a typical size found in experiments, usually well in excess of the coherence length. As for the PSC voltage jump at the onset $I = I_c$, it is expected to be approximately equal to the voltage drop of a current $I_c/2$ in a length 2Λ, or equivalently I_c in a length Λ of normal material.

At a certain amount below T_c, heating effects become significant and the temperature, or "longitudinal", mode is also excited in a PSC [11]. However, that does not essentially change the relationship of Λ to τ_E, except for a multiplicative factor of about 1.7 (refer to (11.5) in [1]). Even farther below T_c, phonon trapping is dominant, and the limiting mechanism which determines the quasiparticle relaxation may be phonon escape. As it will be made clear in the following, we believe most of our measurements belong to that regime.

It has been shown in various situations [4, 5] that a long and homogeneous bridge can hold several PSCs, leading to I–V isotherms made up of segments of respective slopes $R_u, 2R_u, \ldots$, joined by equal voltage jumps. Such a series of steps is usually considered a sufficient signature of PSC formation. Scatter in the critical currents may arise from inhomogeneity along the bridge, but also from the interaction between adjacent PSCs [12]. In the present work however, we restrict ourselves to the first of these steps, corresponding to the formation of a single PSC.

A further distinctive property of current-induced PSCs is their finite nucleation time, which is observed when a time step function, instead of a dc current, passes across the superconducting bridge. This sizeable (nanoseconds) "delay time" t_d readily distinguishes a PSC signal from other types of resistive response, such as the presumably instantaneous vortex flow response. By analyzing the order parameter decay on the basis of a time-dependent Ginzburg-Landau (TDGL) equation simplified to the zero-dimensional case (no gradient term), Pals and Wolter [10] arrived at the explicit form

$$t_d(I/I_c) = \tau_d \int_0^1 \frac{2f^4\,df}{(4/27)(I/I_c)^2 - f^4 + f^6} \tag{1}$$

where the prefactor τ_d (for τ related to delay) of the integral was interpreted as the gap relaxation time. It will instead be treated here as an adjustable parameter to fit the experimental delay times. In the definite integral, to be written $F_{\mathrm{PW}}(I/I_c)$, the temperature enters only through I_c. An elaborated version [13] of (1), with temperature

dependent integration boundaries and a numerator of the integrand replaced by

$$2f^4 + 1.65f^5 - 0.5(I/I_c)^2 \tag{2}$$

permits treating the case of delay times comparable to τ_d. The corresponding theoretical ratio t_d/τ_d, which will be written here as $F_{\mathrm{Tk}}(I/I_c)$, has been used to interpret, over a wide range of temperatures, a number of t_d measurements on metallic films [1], and on high-T_c $YBa_2Cu_3O_7$ strips [14].

The first studies on PSCs were performed on actual one-dimensional (1-D) structures, namely those for which a current-carrying state may be considered homogeneous over the cross-section. In principle, transverse dimensions smaller than both the coherence length and the London penetration depth are required. However, there are less restrictive conditions where phase-slip lines are theoretically possible in a 2-D geometry [15] and are observed in strips that do not strictly satisfy the 1-D conditions, including the case of wide films [6, 16].

Current-induced hot spots can a priori be explained much more simply [7]. With the superconductor being idealized by just two states (normal resistivity ρ above T_c; perfect conductivity below T_c), the current-induced HS is a portion of the bridge sustained in the normal state by the Joule effect, and bounded by two thermal "healing fronts" of length η. To simplify the theoretical treatment of the problem, let us first consider small deviations around T_c, and a uniform volumetric heat capacity C and thermal conductivity κ along the bridge. The other relevant parameter is the film-to-substrate thermal conductance per unit area, α, defined as the heat flux density divided by the difference $T - T_b$, where T and T_b are the film and the bath temperatures, respectively. It is then convenient to introduce the characteristic film cooling time τ by:

$$\tau = \frac{bC}{\alpha} \tag{3}$$

where b is the film thickness. Unlike α, or its inverse, the thermal boundary (Kapitza) resistance R_K, τ is largely independent of T at helium temperatures. In addition, it is directly accessible through measurements in the time domain [17]. With these definitions, the healing length is given by $\eta = \sqrt{\kappa\tau/C}$ in the linear approximation of heat transfer. Also let $J_u(T_b)$ be the current density, (in analogy with the scaling current I_1 appearing in (6) of [7]), that would exactly maintain the temperature T_c in a *uniformly heated* film in contact with a substrate at (bath) temperature T_b, so that:

$$\rho J_u^2 = \tau^{-1} C(T_c - T_b) \tag{4}$$

Order-of-magnitude estimates justify the assumptions of uniformity of the temperature across the film thickness, and of negligible departure of the substrate temperature from T_b during the course of sub-microsecond excitations.

Because of the heat conduction across the healing boundaries, a larger current density $J_h(T_b) = \sqrt{2}J_u(T_b)$ is required [7] to sustain an *isolated* HS upon a substrate at temperature T_b. In a voltage-controlled configuration, the hot spot stabilizes at a length quasi-proportional to the applied voltage [18]. On the other hand, in the case of current drive that we consider here, the HS boundaries move with constant

velocities $\pm U$. Still in a linear treatment of heat transfers, the combination of the Joule heating inside the HS, countered by a transverse loss to the substrate, and by longitudinal heat diffusion, leads to a current-dependent front velocity U given by [19]:

$$U = \sqrt{\frac{\kappa}{C\tau}} * \frac{j^2 - 2}{\sqrt{j^2 - 1}} \tag{5}$$

where $j = J/J_u$ is a reduced current density, limited by the condition $J > J_u$. This formula encompasses, not only the positive values of the velocity for $j > \sqrt{2}$, but also the negative ones for $1 < j < \sqrt{2}$, in which case the hot spot experiences regression [20]. In summary, in the transient regime under current drive, the HS response is a linearly increasing (or decreasing) voltage. The case $U = 0$ defines the border-line value $J_h(T_b)$.

The dependence of any of the two currents densities J_u and J_h upon T_b is parabolic near T_c (see (4)). However, far below T_c, where the linear heat transfer model is invalid, one can attempt to make use of the blackbody radiation power density $\sigma_\phi\ (T^4 - T_b^4)$ per unit film area, where σ_ϕ is the Stefan constant appropriate to acoustic phonons, to represent the heat loss through the interface with the substrate. That law derives merely from (a) a phonon volumetric heat capacity $C_\phi = \beta T^3$, with β constant in the Debye regime, and (b) a temperature-independent phonon escape time $\tau_{\rm esc}$. Combining these two assumptions leads to $\sigma_\phi = b\beta/4\tau_{\rm esc}$, which insures a blackbody emission power tangentially consistent with (4) in the limit $T \to T_b$. Note that σ_ϕ and the boundary resistance R_K satisfy the relationship $4\sigma_\phi T^3 R_K = 1$. Far from the critical temperature, J_u should now follow

$$\rho J_u^2 = \sigma_\phi b^{-1}(T_c^4 - T_b^4) = \beta(T_c^4 - T_b^4)/4\tau_{\rm esc} \tag{6}$$

An estimate of the low-temperature limit J_{u0} obtained through (6) with $\tau_{\rm esc} = 5$ ns (to be justified later), $\rho = 5\ \mu\Omega\,$cm, and $\beta({\rm Nb}) = 135\ \mu{\rm J\,mol^{-1}\,K^{-4}} = 12.3\ {\rm J\,m^{-3}\,K^{-4}}$, deduced from a Debye temperature of 241 K [21], gives $J_u(T_b = 0)$ of around $10^6\ {\rm A/cm^2}$ (we assume that J_{h0}, although larger, is comparable). That value is much less than the low-T critical density limit J_{c0} (see Table 1), which fact forces $J_h(T_b)$ to cross the $J_c(T)$ curve at some temperature T^*. In Fig. 1, the current densities J_c, J_u and J_h are schematically plotted as functions of the temperature, with the understanding that the abscissa for J_c is the *film* temperature T, while J_u and J_h are meant as functions of the *substrate* temperature T_b, a distinction especially relevant when studying hysteresis.

The current-temperature diagram of Fig. 1 allows interpreting the response to *current steps* of increasing amplitude. At $T_{b1} > T^*$, the $J_c(T)$ curve is encountered first, and that defines the proper PSC domain. The interval $T_c - T^*$ was found to be a fraction of a kelvin for tin [4, 5], but a few kelvins for niobium (PSC's far from T_c are reported in [9]), as it will be confirmed shortly. The transformation into a hot spot (HS_1) is expected at a current density $J > J_{h1} = J_h(T_{b1})$, and that is one practical way of determining of the function $J_h(T)$ on the branch $T > T^*$.

At substrate temperature $T_{b2} < T^*$, the $J_u(T)$ curve is met first (point V), but one should not expect any resistance since density J_u corresponds to a decaying

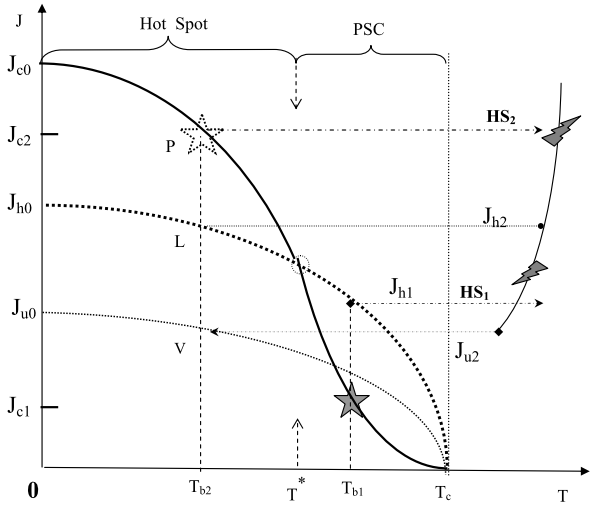

Fig. 1 I–T diagram for 1-D resistive singularities. $J_c(T)$: critical current density. J_u and J_h: threshold densities associated to HS. T_b: bath temperature. T^*: crossing temperature. At $T_{b1} > T^*$, the first response is PSC (star), then a hot spot (HS_1) for $J \geq J_{h1} = J_h(T_{b1})$. Below T^*, point L at $J = J_{h2}$ is passed without response, but the transient PSC excited at J_{c2} (point P) jumps into a growing HS (upward spike HS_2). On reducing J below J_{h2} from that state, HS_2 turns into a receding HS (downward spike). For $J = J_{u2}$, the hot spot collapses uniformly: the bridge returns to point V (zero voltage). Horizontal dash-dot arrows represent fast transitions

HS. Going up in current, it is remarkable that point L is passed with no response, although $J_h(T_{b2})$, here written J_{h2}, be enough to feed a localized HS on a substrate at temperature T_{b2}. Only above the critical density $J_{c2} = J_c(T_{b2})$ does a voltage signal appear. Then the PSC just created, shown as a stippled star, is converted into a hot spot HS_2, which happens to be a spreading HS since then $J > J_c > J_h$. Such behaviour assumes that constant current bias is maintained throughout the process.

If the current amplitude is reduced from that HS_2 state, the velocity of expansion will diminish according to (5), until it falls to zero, and the corresponding value of the current density should define the threshold $J_{h2} = J_h(T_{b2})$. Furthermore, the domain (usually ignored) such that $J_{u2} < J < J_{h2}$ would correspond to hot spots previously created, but having negative values of the front velocity (descending spike in Fig. 1), still in agreement with (5). That situation will be studied in Sect. 5. Eventually, returning to $J < J_{u2}$ below V results in a uniform collapse, rather than a gradual recession, in a time of order τ, commonly a few nanoseconds.

Some control is possible on the parameters that determine T^*, on a given sample. For instance, reducing the critical density, with a lesser effect on the HS threshold J_h, shifts T^* to a lower value. Guided by the I–T diagram only, one could predict the condition for HS ($T_b < T^*$) to become a opportunity for PSC formation ($T^* < T_b$). With that objective in mind, we will examine the influence of an applied magnetic field (Sect. 6).

3 Samples and Experimental Procedures

The specifications of our niobium films are summarized in Table 1, although the measurements ran over a larger number of samples. The FK films were dc-sputtered (2 nm per second) at room temperature on R-plane sapphire wafers, after thorough etching of both the niobium target and the substrate. On the other hand, CV films were made by UHV electron-beam deposition at about 10 nm per second, at room temperature for CV-10 (covered with 5 nm of silicon), and on a substrate heated at 780°C for CV-Al2 (covered with 10 nm of aluminium instead of silicon). The latter procedure results in considerable improvement of the low-temperature mean free path (Second critical magnetic field at 0 K) = 0.965 T in Nb-CV-Al2, instead of 4.6 T in CV-10).

The geometrical and electrical characteristics of the samples are displayed in Table 1, where the low-temperature electronic mean free path l_e is derived from the measured residual resistivity ratio RRR $= \rho(300\ \mathrm{K})/\rho(10\ \mathrm{K})$, and the invariant $\rho l_e = 3.85 \times 10^{-6}\ \mu\Omega\,\mathrm{cm}^2$ [22]. J_c is defined as the minimum current density for PSC or HS formation, whichever occurs first. A resistance versus temperature curve is shown in Fig. 2, for a "dirty" sample taken on the same chip and of the same geometry as Nb-CV-10.

Table 1 Specifications of the niobium strips. Given are the thickness b; width w; strip length; normal state resistivity ρ at 10 K; electron mean free path l_e at 10 K; critical temperature T_c; critical current density J_c at 4.2 K; and resistance per unit length $r = \rho/wb$

Sample	Thickness b (nm)	Width w (μm)	Full length (mm)	ρ (10 K) (μΩ cm)	l_e (10 K) (nm)	T_c (K)	J_c (4.2 K) (MA/cm^2)	r (10 K) (μΩ/μm)
Nb FK-91	80	10	3	2.68	14.5	8.60	4	35
Nb FK-92	80	5	3	4.32	8.9	7.90	3	110
Nb CV-10	100	8.5	0.8	12.1	3.2	8.92	10	140
Nb CV-A12	100	10	3	0.59	65	9.01	11	6.0

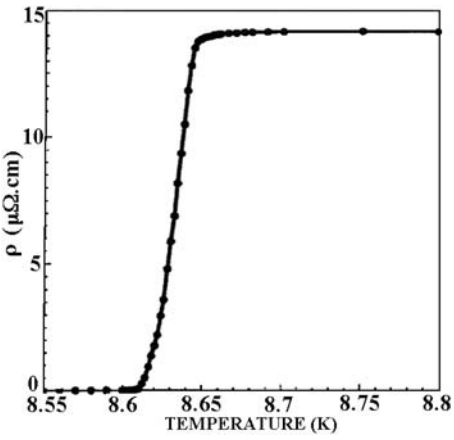

Fig. 2 Superconducting to normal resistive transition $R(T)$ in a filament taken on the same chip as Nb-CV-10

The linear bridge pattern, usually including lateral voltage probes, was obtained through standard photolithography (5214-E positive resin), followed by reactive ion etching in SF_6 plasma. The sample electrodes consist of evaporated gold pads, about 200 nm thick, to enlarge and protect the electrode terminals. An important figure is the resulting contact resistance R_0 (a figure subject to deterioration over the long term, i–e months), which must be kept in the range of 100 mΩ, or less, in view of the strong currents involved in this work. R_0 does not in principle appear in four-points measurement, unless the resistive spot arises, not between the side electrodes, but between one side electrode and the ground terminal. In that case, the sample is not necessarily rejected provided the voltage $R_0 I$ is easily identified (cf. Fig. 6 for instance), and can be subtracted from the total signal without ambiguity.

The system providing the electrical pulses has to meet several requirements: (a) flatness of the pulse shape (to within 1% as far as possible); (b) fine adjustment of the current amplitude; (c) accurate definition of the ratio I/I_c; and (d) constant-current biasing throughout duration of the pulse. An avalanche-transistor generator such as PPL #2600 delivers rectangular signals with sub-nanosecond rise time, and amplitude adjustment by 1-dB steps. To fill the gap between that discrete 1-dB scale and the desired current (condition (b)), the strongly attenuated output of a conventional analog generator (TTL or vacuum-tube, such as Ferisol #301A) was added through a coaxial matched-T. The 50-ohm coaxial feeder circuit includes a low-loss air delay-line (150 or 250 ns) to separate the input pulse from the reflected one and thus allows monitoring the time-varying impedance of the sample by reflectometry. We note that the rather long geometry of our samples is in part responsible for the initial inductive spike present in the recorded signals.

Fulfillment of condition (c) is difficult in the pulse mode and cannot rely upon separate measurements of I_c and I. The critical current I_c is well defined (even if not *known* to the same accuracy) in practice as the pulse amplitude associated with the longest accessible PSC delay time (commonly 500 ns). Then calibrated coaxial attenuators in 0.1 dB steps are successively removed to provide the desired values of the ratio I/I_c. (1 dB corrresponds to a current ratio of 1.122.)

In some cases, direct feeding of the samples by a 50 Ω cable fails to satisfy condition (d) on current biasing. More precisely, the rising HS signal appears gradually as sub-linear in time beyond a sample resistance of about 3 Ω, and eventually goes to saturation at around 8 Ω. To correct for that deviation from the controlled-current condition, a series resistor is inserted in the current feeder close to the thin film sample, and the lateral voltage probes are connected to the output circuitry via 150 Ω resistors.

The measurements were performed either directly in the liquid helium bath, especially for the magnetic field case, or in an evacuated cell provided with an electronic control of the temperature. Because the experiments were carried out in pulse mode, and because the volume of the substrate is thousands of times the film volume, the substrate temperature is assumed to remain unchanged over a pulse duration.

4 Discrimination of PSC, HS and VF Modes in the Transient Regime

In the following, current-induced PSCs will be identified by their nanosecond nucleation delay and the time independence of their voltage. On the other hand, a HS (in constant-current drive) gives rise to a linearly increasing, or decreasing, voltage.

Our method departs from the usual direct-current approach in two essential ways: (a) electrical excitation is applied in the form of step functions of the time and (b) current biasing is maintained as much as possible. It is then straightforward to distinguish the two modes of dissipation, as is attested in Fig. 3, which contrasts the resistive responses of HS at low T and PSC at 5.8 K. Here, one should ignore the initial inductive peak and the subsequent ringing caused by the current leads, as well as the small steady voltage, likely to be caused by a ground contact resistance $R_0 \sim 70\ \mathrm{m}\Omega$. Not only the flat PSC voltage of trace 1, occurring after a delay time $t_d \sim 220$ ns, but also the HS signals (traces 2 and 3), are preceded by a zero voltage period. To our knowledge, this is the first explicit report in the literature of a hot spot nucleation time.

In order to evaluate the critical current, one must look for the current producing an infinite delay or, in practice, the longest t_d compatible with the length of the coaxial delay line (500 ns). This should not entail too severe an error on I_c since t_d is a divergent function of the ratio I/I_c as it approaches unity. According to (59) of [13], in the limit of long delays ($t_d \gg \tau_d$), t_d follows the asymptotic approximation $I(t_d)/I_c = 1 + (\pi\tau_d/t_d)^2$, where $I(t_d)$ is the current that produces the delay t_d. If 10 ns is considered a safe upper boundary for τ_d, we see that $I(t_d = 500\ \mathrm{ns})$ does not exceed I_c by more than 0.2%. Unless explicitly stated, that will be our definition of I_c in the following discussion.

As with PSCs, the HS nucleation time is very sensitive to the current amplitude, and can be quantitatively analyzed in a similar manner. This concerns a statement to be justified later, that both types of resistive centers *derive from the same original process* and accordingly, their delay times are not expected to behave differently.

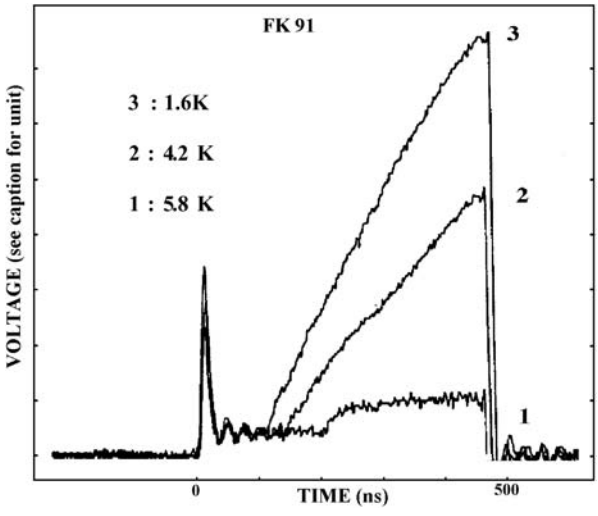

Fig. 3 Time dependence of voltage across FK-91 bridge fed with current steps. Trace 1 (current 21.7 mA; 3.35 mV/vertical division): PSC signal (≈1.9 mV) nucleated at time $t_d = 220$ ns. Traces 2 (33.5 mA; 7.10 mV/div) and 3 (39.2 mA; 7.10 mV/div) display quasi-linearly increasing voltages, characteristic of hot spots. The initial inductive peak and following ringing are inessential features

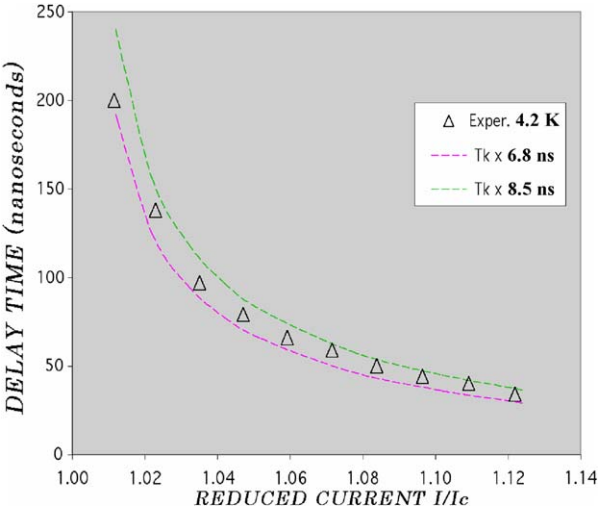

Fig. 4 (Color online) Delay times vs I/I_c (*open triangles*) in Nb-CV-10. *Broken lines*: Function $F_{\mathrm{Tk}}(I/I_c)$ according to (1), (2) for $T/T_c = 0.47$ multiplied by two values of the prefactor τ_d (see insert)

Figure 4 compares HS delay times measured at 4.2 K, for currents not exceeding $1.122I_c$, with theoretical expectations computed from the Tinkham solution F_{Tk} (2). In that range of currents, F_{Tk} $(T/T_c, I/I_c)$ is little sensitive to temperature. Incidentally, it does not depart from the Pals & Wolter function F_{PW} (1) by more than 15% at $I = 1.122I_c$. As one can see, it is possible to bracket the data within two close choices of the prefactor $\tau_d = 6.8$ ns and 8.5 ns. (The two theoretical curves were shifted to the right by a factor 1.002 to compensate for the slight overestimation of I_c explained above.)

If a value such as $\tau_d = 7.5 \pm 0.5$ nanoseconds gives a correct fit to the experimental data, a serious question arises as to its significance, since it does not correspond quantitatively to any microscopic electron relaxation time at 4.2 K. In addition, we hardly observe any variation of τ_d with temperature, or with an applied magnetic field, as it was checked on several samples. So, we suspect that it is related to the film cooling time (3), which is of the right order of magnitude. A similar situation was encountered when analyzing the PSC delay times in $YBa_2Cu_3O_7$ bridges [14], where the parameter τ_d appeared at the same time temperature independent, and essentially proportional to film thickness [17]. We will come back to this point (see Appendix).

According to the SBT model [5], a determination of the PSC extension 2Λ would imply measuring the PSC voltage as a function of the current and deriving the differential resistance R_u. Instead, let us perform a quick estimation by assigning the value $I_c/2$ to the excess current I_S. With this choice, one gets the relation $\Lambda = V_{\mathrm{PSC}}/rI_c$, where $V_{\mathrm{PSC}} = 2.22$ mV is the PSC plateau voltage (trace 1 of Fig. 3) for a current just above I_c, that is for long delay times, and r is the normal resistance per unit length as it appears in Table 1. For sample FK-91 at 5.8 K, where $r = 35$ mΩ/μm, one thus finds $\Lambda \approx V_{\mathrm{PSC}}/rI_c = 3.0$ μm. This in turn determines, through $\Lambda = (v_F l_e \tau_R/3)^{1/2}$ plus $v_F = 0.62 \times 10^6$ m/s, and $l_e = 14.5$ nm taken from Table 1, an inelastic lifetime $\tau_R \sim 3$ ns, another figure incompatible with any pure electronic relaxation time at 4.2 K. Our feeling is that, for τ_R as well as for τ_d, the relaxation processes are dominated by phonon trapping (see Appendix).

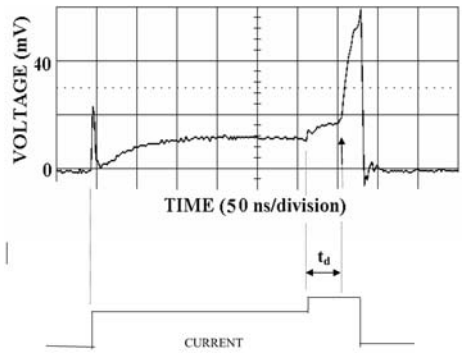

Fig. 5 Transient resistive response of Nb-FK-91 to the current pulse schematized in lower graph in the presence of a perpendicular magnetic field ($T_b = 4.2$ K; field $\perp 60$ mT). At low current ($I_1 = 20.5$ mA), only the VF voltage (*slow rise*) is present. With an increment in current ($I_2 = 32$ mA), a HS state occurs after a delay $t_d \sim 40$ ns (*arrow*)

In a perpendicular magnetic field, our samples are two-dimensional ($w > \xi$) with respect to flux tube (vortex) penetration and there is a possible interference with the localized dissipation modes, in two ways. Except at very low temperature, the vortex depinning current is usually lower than the pair-breaking current. So, in Fig. 5, a first pulse is sufficient to produce a slowly rising VF voltage. About 270 ns later, a supplementary current step is added to produce a HS signal (linear rise) delayed by some 40 ns. Note the absence of delay associated to vortex depinning. The rather slow ascent of the VF signal is the consequence of a small value of the VF resistivity, as compared to ρ in the normal state. Despite its smallness, that relatively low value comes into competition with the HS signal because it is effective over the entire length of the bridge. As a crude approximation, it can be concluded that a magnetic field has little consequence on, or for the least does not prevent, the formation of hot spots.

Phase-Slip Centers do coexist with the vortex flow as well, and then add themselves to the VF voltage with apparently no interference. So we have observed at 1.5 K, in a modest perpendicular magnetic field (9 mT), two successive PSC signals on top of a VF voltage, identified by its non-delayed slow rise. The presence of PSCs at low temperature, in apparent contradiction with the predictions of Fig. 1, is made possible by the magnetic field itself, as it will be made more explicit in Sect. 6.

A more intricate question would concern the influence of the vortex state on the very nucleation process of PSC or HS. In brief, does the vortex state tend to inhibit, or promote their formation? Let us concentrate on the nucleation time since it is such a sensitive probe of the superconducting response, and summarize very briefly our observations. For given temperature and current, t_d is strongly reduced by a magnetic field, but only to the extent that the current threshold $I_c(H)$ is reduced. As a matter of fact, in a large span of fields, up to 0.7 T, *the HS or PSC delay time keeps the same dependence upon* I/I_c as that displayed in Fig. 4, *provided* I_c *is the critical current appropriate* to the temperature and the magnetic field applied. So, vortices seem to play no more than a passive role on PSC formation except, possibly, in a limited range of fields. Their influence amounts here to a reduction of the sample width.

5 Experimental Determination of the Current-Temperature Diagram

Let us summarize the conclusions of Sect. 2. Proceeding with current steps of increasing amplitude at bath temperature $T_{b1} > T^*$, one first crosses the $J_c(T)$ curve, which

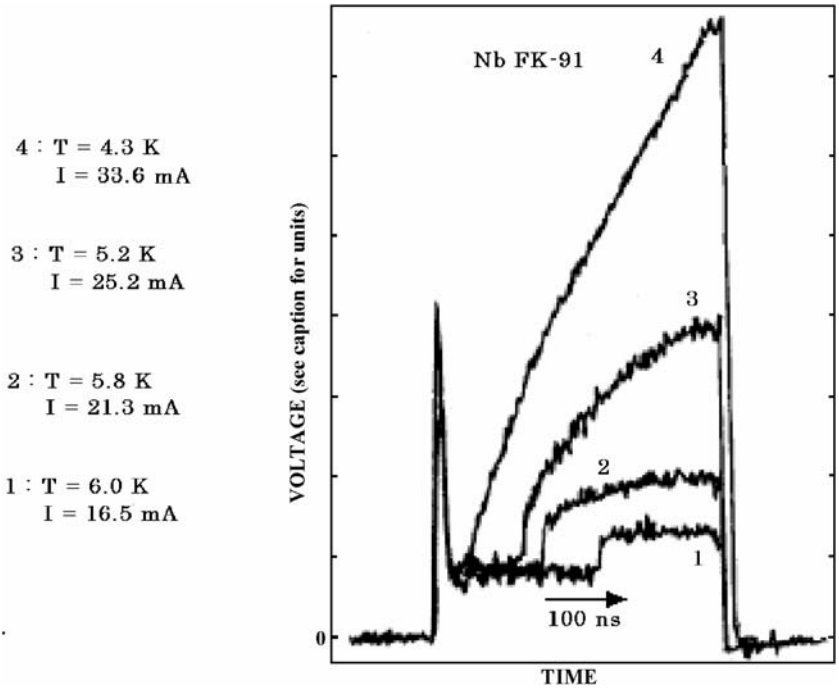

Fig. 6 Time dependence of voltage across Nb bridge FK-91 for several conditions of temperature and current. Compare the flat PSC signal (1) to the linearly rising HS voltage (4). From their position with respect to T^*, we interpret Trace 2 as a PSC signal with strong heating and Trace 3 as a HS signal fed with a current slowly decreasing with the time. (See text.) Vertical sensitivities in millivolts per division are: (1) 1.90; (2) 1.94; (3) 2.15 and (4) 4.45

leads to a resistive response in the form of one (Fig. 3, trace 1; Fig. 6, trace 1), or possibly several PSCs with voltage(s) stable in time. If the current density $J_{h1} = J_h$ (T_{b1}) is exceeded, the conditions are met for the transformation of a PSC into a growing HS. Then, a hot spot (not shown here) results, usually with a short delay time if J_h is significantly larger than J_c. That allows measuring both J_c and J_h above T^*.

On the other hand, the first observed low-T response is invariably a growing hot spot, itself preceded by a well-defined delay, as in Fig. 3 (traces 2 and 3), Fig. 6 (trace 4) and Fig. 7. It must be noted that a plot of the current density giving the *first response* shows no discontinuity of slope at any T throughout the full superconducting range. Actually it is a plot of the critical $J_c(T_b)$, consistently with the fact that, in all cases, a PSC has been excited first. The conversion of PSC into HS is more gradual in the vicinity of T^* (traces 2 and 3 of Fig. 6).

A better illustration of the passage through a transient PSC state is obtained using a mounting of the superconducting bridge designed for the observation of short rise times (Fig. 7). From direct inspection, the characteristic HS linear ramp appears preceded at time t_d by an abrupt voltage step which, plausibly, is the transient PSC response, on the basis of two arguments: (a) the delay time of this signal follows the delay function $t_d(I/I_c)$ formerly detailed in (1), (2), and (b) its amplitude ΔV

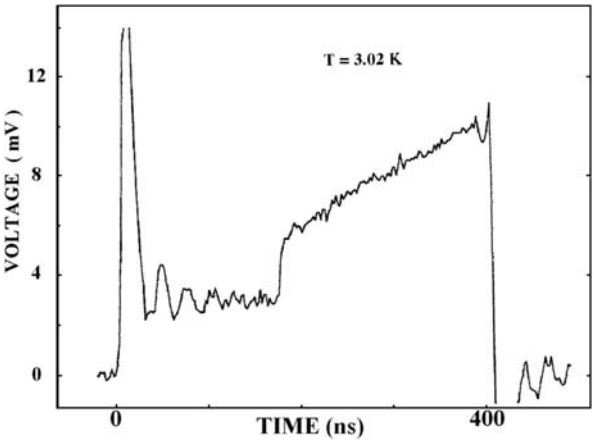

Fig. 7 Voltage response *vs* time of FK-91 at $T_b < T^*$. Current step: 35.4 mA. The sudden rise at $t_d \approx 180$ ns is assigned to PSC nucleation, the following linear rise to HS growth. Short rise times are responsible for the large inductive spike and ringing

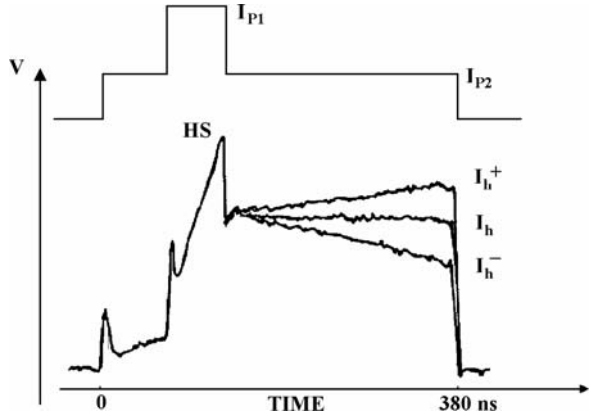

Fig. 8 Voltage responses *vs* time of Nb bridge FK-91 at $T_b = 5.2$ K for three close values of the return current I_{P2} (lower traces). The current $I_{P2} = I_h$ which sustains a stable response defines the HS threshold current I_h. *Upper graph*: Temporal pattern of juxtaposed current pulses I_{P1} and I_{P2}

is in sound proportion with the voltage step V_{PSC} measured in the proper PSC domain $T > T^*$. (In Fig. 7 the equivalent resistance $I^{-1}\Delta V$ is 52.7 mΩ, not far from $I^{-1}V_{\mathrm{PSC}} = 57.5$ mΩ in trace 1 of Fig. 6.) Soon after t_d, in a time of order τ, and because $J_c > J_h$ at $T_b < T^*$, the PSC in its center is likely to be driven above T_c, and therefore switches into a hot spot.

To go further with interpretation, let us conclude that a hot spot does not appear at $J = J_h$ as a consequence of a temperature fluctuation of amplitude $\Delta T > T_c - T_b$, or it would otherwise appear randomly in time, or at any location along the bridge. Neither can it be the result of slow Joule heating of some residual resistance, since it obeys the PSC delay law (1), (2). Rather, it necessitates the more fundamental PSC mode for ignition. So, a point such as L ($T_b < T^*$; $J = J_h$) in Fig. 1 *represents a latent HS inaccessible directly by a single step of current*. It will be shown now that L can be reached "from above" once a HS has been produced by other means, as suggested by the trajectory $\mathrm{HS}_2 => J_{h2} => L$ drawn as a dotted line.

Experimentally, this is achieved by the superposition, on top of the principal current pulse, of a second short step (Fig. 8, upper trace), large enough to reach $I_c(T_b)$

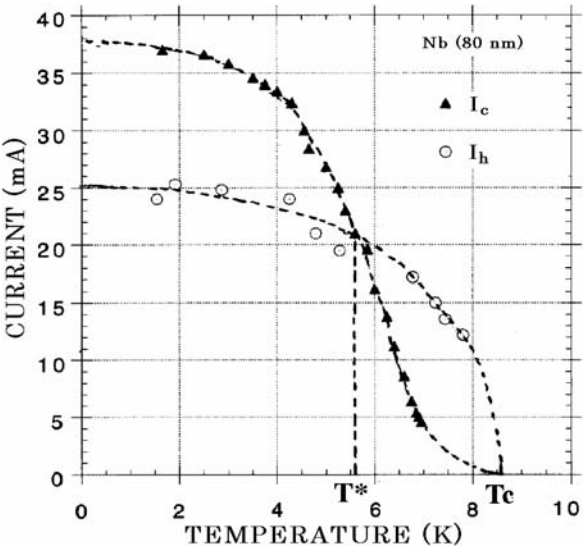

Fig. 9 Temperature dependence of the threshold currents I_c and I_h measured in niobium strip FK-91. Intersection at $I = 21$ mA and $T^* = 5.65$ K. The data for I_h are obtained by using the two-step pulse technique described in text

and therefore to produce a growing HS through a transient PSC state. Then, the current is reduced to a stationary lower value, with three possible outcomes: increasing, decreasing, or steady voltage, according to the current I_{P2} selected, I_h^+, I_h^- or I_h respectively. The latter case defines the threshold hot spot current $I_h(T_b)$, and so the point $L(T_b)$ can be plotted in the I–T diagram. (A return from HS to a PSC state is also possible. This point will be examined in Sect. 7.) The definiteness of that determination of I_h can be appreciated as follows: in the conditions of Fig. 8, if we call V_{HS} the hot spot signal, the HS front velocities $U = (1/2rI)(dV_{\mathrm{HS}}/dt)$ under the currents I_h^+ and I_h^- are respectively $+$ and -8 m/s, to be compared with a scaling velocity $\sqrt{\kappa C/\tau}$ of several hundred of m/s. On the basis of (5), this is equivalent to say that the side currents differ by no more than a few parts per thousand and so it is reasonable to state that I_h is *defined* within about 0.2%, even if a *measurement* of the pulsed current I_{P2} does not reach that level of accuracy.

Below the current I_h (or below the current density J_h) is the finite domain of negative HS front velocities: $I_u < I < I_h$. On lowering the intensity I_{P2} of the return current pulse, the HS retraction becomes faster and faster until the decrease of the voltage is no longer linear in time. Instead, the hot spot collapses uniformly in a time of order τ. That minimum of I_{P2} defines $J_u(T_b)$.

Results for currents I_c and I_h measured in niobium bridge FK-91 are plotted in Fig. 9 as a function of temperature. The crossing temperature is $T^* = 5.65$ K, that is, much farther from T_c than was found for tin [3–5]. In this graph, the interpolation between experimental data (dotted lines) was drawn by visual adjustment, and not supposed to follow a definite algebraic law. It was extended towards T_c so as to fit a horizontal tangent at T_c for the critical current, and a vertical tangent for the hot spot current.

6 Magnetic Field. Predictions from the I–T Diagram

In the last two sections, we wish to test the effectiveness of the I–T diagram with respect to external agents influencing the superconducting state, without addressing the exact nature of the perturbation though. A magnetic field acts in many ways, which all lead to a weakening of the superconductivity. In an I–T representation of this problem (Fig. 10a), the depressed critical temperature T_c', dependent upon the field strength H, is shown accompanied by a decrease of both the critical current $I_c'(T)$ and of the minimum HS current $I_h'(T)$. Correspondingly, the crossing temperature in a field shifts to a lower value $T'^*(H)$. At an intermediate bath temperature $T'^* < T_b < T^*$, the inequality relation between I_c and I_h in a field is reversed compared with the zero-field situation. As a consequence, the first resistive response to current pulses of increasing amplitude is expected to pass from HS in zero-field, to PSC in the field H, along the vertical line belonging to temperature T_b.

Experimentally, we restrict ourselves to the perpendicular geometry, and to temperatures low enough for vortex motion to be frozen, in order to avoid an interference of the pair-breaking current I_c with the irrelevant vortex-depinning current. The zero-field response of sample CV-Al2 (top trace of Fig. 10b) is of the HS type and

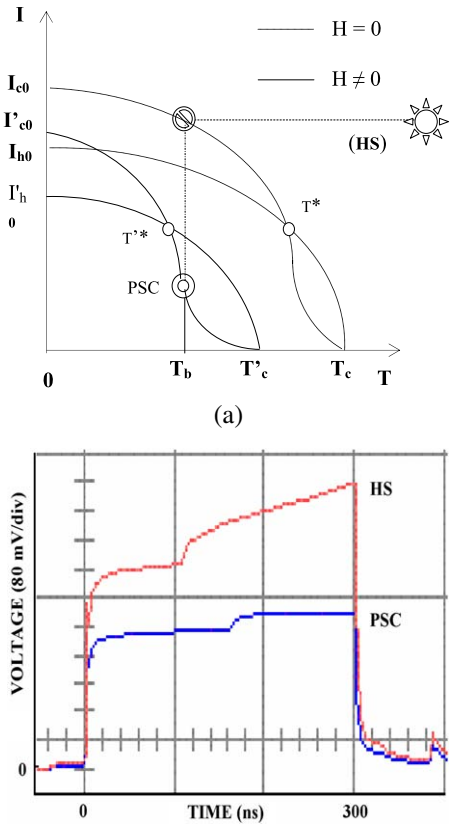

Fig. 10 (**a**) I–T diagram in a (*perpendicular*) magnetic field (*continuous curves*), compared with the zero-field *dotted curves*. The crossing temperature is reduced from T^* to T'^*. At an intermediate substrate temperature T_b, the diagram for $H \neq 0$ predicts a PSC response instead of a hot spot (HS) in zero field. (**b**) (Color online) Effect of a perpendicular magnetic field on the resistive response of Nb-CV-Al2 at 1.5 K. Top graph (zero field; $I_c = 107$ mA): HS response (linear rise). *Lower graph* ($H = 10$ mT; $I_c = 87$ mA): PSC response. Both signals appear retarded by a long delay, on top of a plateau arising from a 0.8Ω-contact resistance. The vertical scale takes account of the 150Ω-series resistors

indicates, after conversion of voltage into an equivalent length of normal material, the formation of a resistive zone growing at the velocity $2U \sim 68$ m/s. In contrast, the lower trace (non-zero field) displays the flat PSC pattern, corresponding to a normal length $2\Lambda = 10.2$ μm. (Because of a defective contact at the ground electrode, and because the singularity occurs near that electrode, there exists a constant plateau voltage which should be mentally subtracted from each of these signals. On the other hand, the signals are free from the initial inductive spike thanks to a 50 ohms-resistor mounted in series with the feeder line.) In both cases, the mere presence of a delay certifies that the bridge is in (or, in the HS case, has transited stealthily through) a PSC state. The long delay times ($t_d > 100$ ns) insure, in each case, that the pulsed current is only slightly superior to the critical value $I_c(H, T)$. So, the change of response, between the zero-field and the $H \neq 0$ situation, confirms the expectations drawn from Fig. 10a.

7 Response to a Uniform Light Pulse

Light falling onto a metal film is partially absorbed, by way of photon-electron collisions that take place on the femtosecond scale. Then, within picoseconds, the energy of the excited electrons relaxes towards the electron and phonon systems, so that an effective temperature can approximately describe the situation [23], except possibly for a limited range of long-wavelength phonons. A temperature jump is therefore a simple, not so inexact, way of rendering the effect of light irradiation, at least on the time scale pertinent to the phenomena considered in this paper (nanoseconds). The temperature excursion ΔT following the absorption of a short light pulse can be determined from the light intensity and the film cooling time.

We have exposed niobium bridges to *fixed* light pulses, synchronized with rectangular electrical pulses, slightly sub-critical in the absence of light, acting as a controlled-current bias. A cavity-dumped argon ion laser was used to deliver unfocused pulses about 30 ns long (20 ns at mid-height) which raise temporarily the temperature of the whole film by ΔT, without substantially heating the (transparent) sapphire substrate. Any localized resistive state is likely to appear where it would have in the absence of irradiation, but this does not affect the interpretation to follow. The laser power is adjusted in such a way that there is no resistive response at small bias current, to insure that the film has not been heated above T_c during irradiation. As a function of the current intensity carried in the bridge, we find the three types of voltage response displayed in Fig. 11b.

According to the conclusions of Sect. 5, creating a resistive state requires the bias current to pass over the critical value at the relevant temperature. This amounts to requiring that the points of coordinates $(T_f = T_b + \Delta T,\ I_k)$ be located in the (I, T) diagram (Fig. 11a) on the upper-right side of the $I_c(T)$ curve. (I_k's with $k = 1, 2, 3$, refer to the three bias pulse amplitudes selected.) The top trace ($I_3 = 64$ mA) of Fig. 11b, which clearly bears the signature of a growing hot spot, implies that I_3 exceeds the HS threshold current $I_h(T_b)$. The transient PSC (Point 3) is converted into a HS state of central temperature $T_M > T_c$. Note that the substrate temperature T_b, not the film temperature, is here the relevant parameter to define I_h. Incidentally,

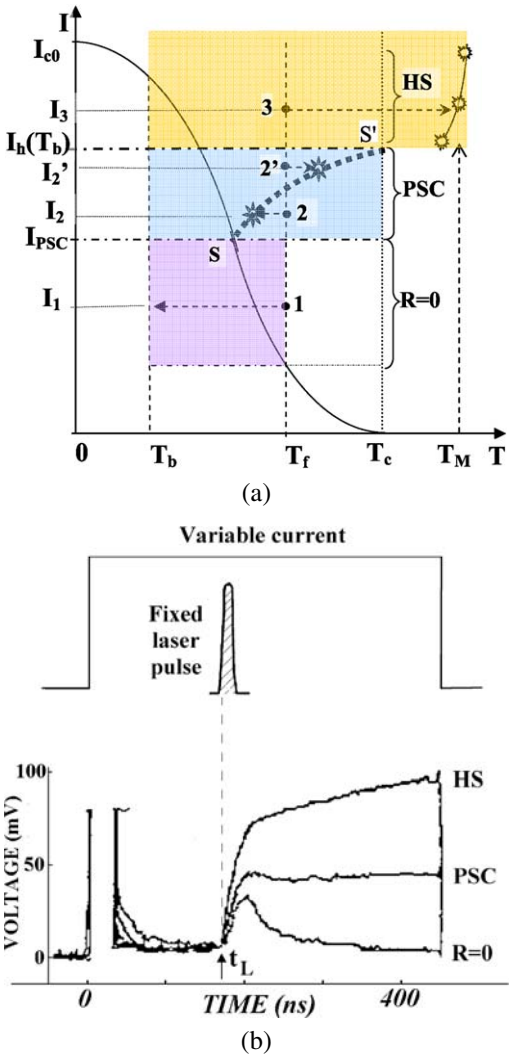

Fig. 11 (**a**) (Color online) I–T diagram for a superconducting bridge, initially at $T = T_b$, launched to T_f by a laser pulse. According to the bias current, the evolution proceeds to $R = 0$ (bias current I_1), PSC (I_2; I_2'), or growing HS (bias I_3). Current $I_h(T_b)$ is the HS threshold while arc SS′ is a plausible I–T relationship for a durable PSC. Points 1 and 3 represent transient PSC states. (**b**) Response *vs* time at $T_b = 1.9$ K of niobium strip FK-91 to combined sub-critical rectangular pulses of current (starting at time 0) and laser pulses (schematized) falling at time t_L. The three waveforms labeled $R = 0$, PSC, and HS correspond respectively to the 3 values of current $I_1 = 50$ mA, I_2 around 60 mA, and $I_3 = 64$ mA, all below $I_c(T_b)$. *Top graph*: current and laser temporal patterns

I_3 must be lower than $I_c(T_b)$, since by assumption it has not induced a voltage by itself.

Below $I_h(T_b)$, Joule dissipation inside the freshly created PSC is by definition not sufficient to raise the film temperature up to T_c. However, the PSC dissipates a power $\rho J[J - J_S(T)]$ per unit volume, with a core temperature (see (8) in Appendix) tentatively represented by the arc of curve SS′ in Fig. 11a. Then, for currents I_2 and I_2', the initial states 2 and 2′ move to the permanent states represented as suns. Correspondingly, the intermediate trace (bias current $I_2 \sim 60$ mA) of Fig. 11b which, apart from a very small overshoot, is a voltage constant in time, should be assigned either to a PSC response, or to a HS exactly biased at $I_h(T_b)$. Since there is, not a single value, but a range of bias currents around 60 mA giving essentially the same picture, one must favor the PSC interpretation.

However, there is a minimum bias, namely I_{PSC}, for which Joule dissipation is unable to sustain the film temperature above the $I_c(T)$ curve (limiting point S in Fig. 11a). Then, the transient PSC state initiated at a point such as 1, should vanish in agreement with the status of PSC as the minimum dissipation unit [5], and the film should return to the uniform $R = 0$ state at temperature T_b. The lower trace of Fig. 11b ($I_1 = 50$ mA) shows such a transient signal returning to zero at a pace determined by the bias current intensity.

8 Conclusion

A long superconducting strip is found to exhibit the resistive singularities known in one-dimensional structures, namely phase-slip centers and hot spots, which are identified here from the transient voltage following a sudden current excitation. Thanks to a double-pulse technique, the HS response can be displayed in its growing, stable, or regressive phase. It is shown for the first time that the HS formation is preceded by the delay characteristic of PSC nucleation. Indeed, a HS does not arise spontaneously, but rather necessitates the rapid passage through a PSC state to overcome the thermal energy barrier. Conversely, it is possible to generate PSC states at virtually any temperature by the sudden quenching of a hot spot.

All these evolutions can be depicted in a current-temperature plane containing a plot of the functions $I_c(T)$ and $I_h(T)$. A well-defined "crossing temperature" T^* separates the PSC domain near T_c, from the low-temperature domain, where the first response to currents of increasing amplitude is a hot spot. Such a diagram has some predictive power: in the presence of a magnetic field, the HS first response can turn into a PSC first response. That is in agreement with the magnetic decrease of T^*, even if it ignores the details of the influence of the external agent. In response to an incoming "temperature" pulse, realized by a uniform laser excitation, the behaviour of a filament is determined by the working point selected in the I–T plane. As a consequence, the result may be a transient voltage, bound to terminate at zero level, a constant voltage (PSC), or an unbounded signal (growing HS). It must be noted that the extreme case of single-photon detection in ultrathin NbN strips [23] was interpreted differently, not as a temperature pulse, but instead as an increment of the current density induced by the squeezing of the current lines.

In an attempt to represent, over a wide span of temperature (i–e far from T_c), the state of excitation reached inside the resistive spot, the film-to-substrate heat transfer was introduced in order to evaluate the amount of heating (Appendix). Quantitatively, the assumption of a phonon blackbody radiation-law proves superior to a linear model of heat transfer. Let us note that our phonon escape times, common to both models, do not rely on quasi-static heat transfer measurements, but rather were inferred from the observed PSC nucleation times.

In some conditions, vortex flow can coexist with the present localized modes, but the possible interference with PSC nucleation is a problem still to be solved.

Acknowledgements The Laboratoire Pierre Aigrain (LPA) is a "Unité Mixte de Recherche ENS-CNRS-UMR 8551", associated with Universities Paris 6 and Paris 7. This work was supported by contracts ACI DESIQ 2003 and C-Nano IdF DSEPU 2007.

We are indebted to C. Delalande (LPA), B. Pannetier (CRTBT, Grenoble), Roger W. Bland (SFSU San Francisco), and Phan Hong Khôi (VAST HàNôi), for their constant interest. We also thank Sukhee Dhillon (LPA) for his reading of the manuscript.

Appendix: Delay Time, Boundary Resistance, and PSC Heating

In connection with the PSC delay times (Fig. 4), it was proposed that the prefactor τ_δ of the $t_d(I/I_c)$ function (1, 2) be identified with a film cooling time (τ), when this time takes the place of the inelastic electron-phonon lifetime [11], i–e well below T_c. However, the heat transfer to the substrate is taken up by the phonon system only. Therefore, if $\tau_{\rm esc}$ denotes the phonon escape time, and if the specific heats of phonons C_ϕ and of electrons C_e add up to $C = C_\phi + C_e$, there results $C_\phi/\tau_{\rm esc} = C/\tau$. By direct inspection of specific heat data (Fig. 1 of [21]) in the S state, we read $C(4.2\ {\rm K}) = 31.2\ {\rm mJ/mol\,K}$ and, from the normal state data, $C_\phi(4.2\ {\rm K}) = 10.0\ {\rm mJ/mol\,K}$. One then obtains $\tau_{\rm esc} = (C_\phi/C)\tau_d = 2.5$ ns for film CV-10 of thickness $b = 100$ nm. Applying finally a rule of proportionality to thickness, one obtains for Nb films sputtered on polished sapphire the phonon escape time per unit thickness:

$$\frac{\tau_{\rm esc}}{b} = 25\ \frac{\rm ps}{\rm nm} \tag{7}$$

equivalent to a heat boundary resistance $R_K({\rm Nb/R\text{-}Al_2O_3}) = \alpha^{-1} = \tau_{\rm esc}/bC_\phi = 20\ {\rm T^{-3}\,cm^2\,K^4/W}$. An attractive feature of the present determination of τ is to have been performed *in the superconducting* (S) *state*. $\tau_{\rm esc}$ should not vary significantly with temperature for the long-wavelength acoustic phonons involved here. A similar procedure, checked in great detail for the case of $YBa_2Cu_3O_7$ films deposited on (100) MgO [17], led to the result $\tau_{\rm esc}/b = 75$ ps/nm.

We are now in a position to estimate the temperature inside a self-heating singularity, if we assume that a single temperature can describe the state of the filament at a given abscissa. Let us consider a well-developed hot spot, i–e much longer than twice the healing length, and its central temperature T_M. (The healing length $\eta = \sqrt{R_K b\kappa}$, in which the thermal conductivity κ can be derived from the Wiedemann-Franz law, is about 1.5 µm near T_c in sample FK-91.) Due to the flatness of the temperature profile around the center [18], the heat loss is almost entirely carried by phonon escape to the substrate, and very little by diffusion along the filament. In the case of trace 4 ($T_b = 4.3$ K; $I = 33.6$ mA) in Fig. 6, a linear model of heat transfer would yield $T_M - T_b = R_K \rho I^2/w^2 b = 102$ K, quite an unrealistic result. Clearly, the substantial temperature difference with the substrate makes it impossible to assign a proper value to R_K. If instead we balance the Joule heat transferred per unit film area $\rho I^2/w^2 b$ with the blackbody radiation power $\sigma_\phi(T_M^4 - T_b^4)$, as in (6), we obtain for the central HS temperature the plausible result $T_M = 13.5$ K, not far from symmetrical of T_b with respect to T_c. We remark the great efficiency of the blackbody radiation for the control of the temperature rise. (A similar computation, applied to trace 3 at $T_b = 5.2$ K, yields $T_M = 11.6$ K.)

In order to adapt this type of reasoning to the localized PSC structure, let us follow the procedure of Kadin et al. [11], who consider that the heat transferred to the

substrate, plus the heat conducted along the filament, is equivalent to a total power V.I dissipated over a strip length 2 $(\eta + \Lambda)$ raised at the core temperature T_m, so that:

$$2(\eta + \Lambda)w(T_m - T_b) = R_K V I \tag{8}$$

Out of the several traces displayed in Fig. 6, trace 1 at $T_b = 6.0$ K would correspond to $\Lambda \approx 2.8$ μm (assuming $f = 1/2$), and $\Delta T = T_m - T_b \sim 0.7$ K. For the larger ΔT expected at $T_b = 5.8$ K (trace 2), the lack of knowledge on the actual critical current at temperature T_m makes any estimate uncertain, but for the fact that T_c stands as a safe upper bound on T_m. Due to the rapid decrease of I_c on approaching T_c, the limiting case $f = 0$ is not unlikely. An estimate of ΔT according to (8), assuming $f = 0$ and a boundary resistance R_K computed for $T = T_c$, yields a temperature elevation of (2.5 ± 0.5) K, that is a core temperature close to T_c. The PSC signal of trace 2 shows indeed clear signs of divergence. In practice, it was the maximum amplitude that could be observed before the PSC is converted into a HS (trace 3).

References

1. M. Tinkham, *Intro. to Superconductivity*, 2nd edn. (McGraw-Hill, Singapore, 1996), Chap. 11
2. T.J. Rieger, D.J. Scalapino, J.E. Mercereau, Phys. Rev. B **6**, 1734 (1972)
3. W.W. Webb, R.J. Warburton, Phys. Rev. Lett. **20**, 461 (1968)
4. J.D. Meyer, App. Phys. **2**, 303 (1973)
5. W.J. Skocpol, M.R. Beasley, M. Tinkham, J. Low Temp. Phys. **16**, 145 (1974)
6. A.G. Sivakov, A.M. Glukhov, A.N. Omelyanchouk, Y. Koval, P. Müller, A.V. Ustinov, Phys. Rev. Lett. **91**, 267001 (2003)
7. W.J. Skocpol, M.R. Beasley, M. Tinkham, J. Appl. Phys. **45**, 4054 (1974)
8. G.J. Dolan, L.D. Jackel, Phys. Rev. Lett. **39**, 1628 (1977)
9. R.B. Laibowitz, A.N. Broers, J.T.C. Yeh, J.M. Viggiano, App. Phys. Lett. **35**, 891 (1979)
10. J.A. Pals, J. Wolter, Phys. Lett. A **70**, 150 (1979)
11. A.M. Kadin, W.J. Skocpol, M. Tinkham, J. Low Temp. Phys. **33**, 481 (1978)
12. J.M. Aponte, M. Tinkham, J. Low Temp. Phys. **51**, 189 (1983)
13. M. Tinkham, in *Non-Equilibrium Superconductivity, Phonons and Kapitza Boundaries*
14. F.S. Jelila, J.-P. Maneval, F.-R. Ladan, F. Chibane, A. Marie-de-Ficquelmont, L. Méchin, J.-C. Villégier, M. Aprili, J. Lesueur, Phys. Rev. Lett. **81**, 1933 (1998)
15. A. Weber, L. Kramer, J. Low Temp. Phys. **84**, 289 (1991)
16. V.G. Volotskaya, I.M. Dmitrenko, A.G. Sivakov, Sov. J. Low Temp. Phys. **10**, 179 (1984)
17. K. Harrabi, N. Cheenne, F. Boyer, F. Chibane, P. Delord, F.-R. Ladan, J.-P. Maneval, Supercond. Sci. Technol. **13**, 1222 (2000)
18. G.D. Poulin, J. Lachapelle, S.H. Moffat, F.A. Hegmann, J.S. Preston, App. Phys. Lett. **66**, 2576 (1995)
19. A.V. Gurevitch, R.G. Mints, Rev. Mod. Phys. **59**, 941 (1987)
20. V.D. Lam, L.V. Hông, P.H. Khôi, F. Boyer, J.-P. Maneval, Commun. Phys. **13**, 81 (2003)
21. H.A. Leupold, H.A. Boorse, Phys. Rev. A **134**, 1322 (1964)
22. A.F. Mayadas, R.B. Laibowitz, J.J. Cuomo, J. Appl. Phys. **43**, 1287 (1972)
23. G.N. Gol'tsman, O. Okunev, G. Chulkova, A. Lipatov, A. Semenov, K. Smirnov, B. Voronov, A. Dzardanov, C. Williams, R. Sobolewski, Appl. Phys. Lett. **79**, 705 (2001)